Contrasting methods for symbolic analysis of biological regulatory networks

Roy Wilds*
Department of Mathematics and Statistics, McGill University, 805 Sherbrooke Street West, Montreal, Quebec, Canada H3A 2K6

Leon Glass†
Department of Physiology, McGill University, 3655 Promenade Sir William Osler, Montreal, Quebec, Canada H3G 1Y6

(Received 24 April 2009; revised manuscript received 27 October 2009; published 29 December 2009)

Symbolic dynamics offers a powerful technique to relate the structure and dynamics of complex networks. We contrast the predictions of two methods of symbolic dynamics for the analysis of monotonic networks suggested by models of genetic control systems.

DOI: 10.1103/PhysRevE.80.062902 PACS number(s): 87.16.A−, 89.75.Hc, 05.45.Ac, 05.45.Tp

New methods for the analysis of biological networks are leading to a rapid increase in our knowledge about the topology and qualitative interactions between constituent components. For example, recent progress has been made in identifying and analyzing the protein-DNA interactions that control gene expression in yeast [1] and the network connections and interactions between neurons in rat brain [2]. However, a detailed quantitative determination and modeling of the interactions is difficult to achieve. Methods are needed to determine robust features of the dynamics that would be insensitive to the fine details of the interactions over large ranges of parameters. In particular symbolic dynamics [3] provides a perspective for studying biological dynamics. Several groups have presented symbolic methods to capture qualitative aspects of biological interactions and dynamics [4–8].

The current Brief Report is motivated by a recent manuscript that analyzes symbolic dynamics in feedback networks with monotonic interactions [8]. Networks with monotonic interactions are defined by the equations

$$\dot{x}_i = g_i(x_1, x_2, \ldots, x_n), \quad i = 1, \ldots, n, \tag{1}$$

where $\dot{x}_i$ is the time derivative of $x_i(t)$ and if g_i depends on x_j, then $\mathrm{sgn}\frac{\partial g_i}{\partial x_j} \in \{+,-\}$ is constant, where sgn is the algebraic sign function. We say that j activates i if $\frac{\partial g_i}{\partial x_j}$ is everywhere positive; and j represses i if $\frac{\partial g_i}{\partial x_j}$ is everywhere negative. In one example, Pigolotti *et al.* [8] considered a network depicted in Fig. 1(a) in which the dynamics were dominated by the oscillation in the negative feedback loop present when the interaction $3 \to 2$ is eliminated. In what follows, we compare the "derivative discretization" method of symbolic dynamics in Ref. [8] with an alternative "threshold discretization" method [4] by analyzing monotone networks consistent with Fig. 1(a). Although the derivative discretization can be used to place restrictions on transitions for the entire class of monotone networks consistent with Fig. 1(a), for monotone systems with switchlike nonlinearities, the threshold discretization enables a more precise prediction of dynamics, and can be used to predict the existence of limit cycle oscillations and fixed points.

The *derivative discretization* dissects phase space into distinct regions in which the signs of the derivatives are constant [8]. The nullclines of Eq. (1) are the $(n-1)$-dimensional surfaces defined by $g_i(x_1, \ldots, x_n)=0$, for $i=1, \ldots, n$. Thus, in general, the symbolic dynamics can be represented by an n-dimensional hypercube, n cube, where each vertex is labeled by a symbolic state $[\mathrm{sgn}(\dot{x}_1), \mathrm{sgn}(\dot{x}_2), \ldots, \mathrm{sgn}(\dot{x}_n)]$. The directed edges, which represent allowed transitions between symbolic states, can be determined as follows. Consider adjacent vertices A and B such that the symbolic state of the i^{th} component of A and B are different, but all other components are identical between A and B. There is a directed edge from A to B if

$$c_j = \left(\mathrm{sgn}\frac{\partial g_i}{\partial x_j}\right) \times (\mathrm{sgn}\ g_j) \times (\mathrm{sgn}\ g_i) < 0 \tag{2}$$

for any x_j that is an activator or repressor of i. This rule, which is equivalent to the formulation in Ref. [8], is used to generate Fig. 1(b). Using the derivative discretization all symbolic transitions that occur in a monotone network *must* be consistent with the allowed transitions found using this rule, but not all transitions found using this rule will necessarily occur in any given network. By definition, any fixed points must lie outside of the regions of phase space repre-

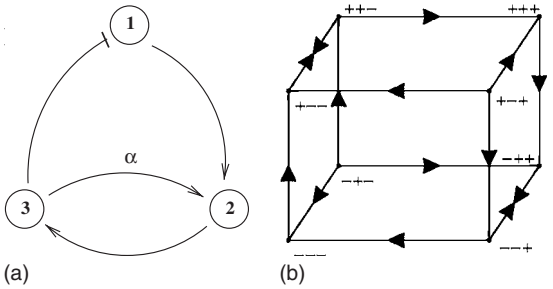

FIG. 1. (a) Interaction diagram for a monotone network studied in Ref. [8]. The edges → represent an activating influence, whereas the edges ⊣ represent an inhibiting influence. The edge labeled by α represents an interaction with variable strength, parameterized by α. (b) The allowed symbolic transitions using the derivative discretization of (a). Vertices (−+−) and (+−+) were omitted in [8].

*wilds@cnd.mcgill.ca
†glass@cnd.mcgill.ca

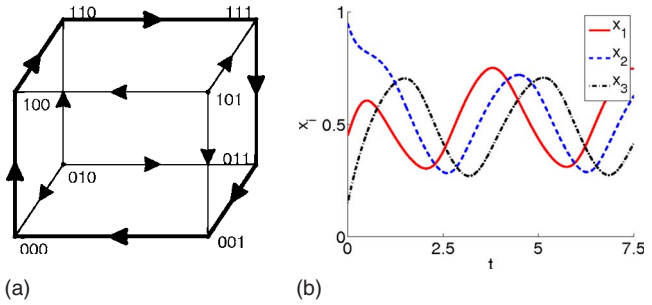

FIG. 2. (Color online) Negative feedback loop Eq. (5). (a) The state transition diagram produced by the threshold discretization. (b) Integration of Eq. (5) with $\eta=5$.

sented by the symbolic states of the derivative discretization. As we show below, vertices such (+−−) in Fig. 1(b) might still identify a region of phase space in which transients asymptotically approach a fixed point even though there is an allowed transition out of the vertex.

The *threshold discretization* provides an alternative method for symbolic dynamics [4]. The threshold discretization partitions the phase space into 2^n sectors. Each sector is labeled by a Boolean vector, $(X_1, X_2, \ldots, X_n)$, $X_i \in \{0,1\}$, where X_i is defined via the Heaviside step function $X_i = H(x_i - \theta_i)$, and θ_i is a threshold. Thus, the dynamics can be represented by a directed graph on an n cube where the directed edges between adjacent vertices represent the allowed flows between neighboring sectors. The directed n cube is called the state transition diagram. The threshold discretization, and resulting symbolic dynamics has been studied for the piecewise linear equations,

$$\dot{x}_i = -x_i + f_i(X_1, \ldots, X_{i-1}, X_{i+1}, \ldots, X_n), \quad i = 1, \ldots, n \quad (3)$$

where the f_i specify the regulation of the i^{th} element. In one special case, the f_i are Boolean functions of the $(n-1)$ inputs defined by the $\{X_i\}$. For Eq. (3), in general the flow across each boundary between two adjacent sectors is transversal and in a unique orientation. Suppose two adjacent vertices A, B differ only in the j^{th} binary value, with vertex A such that $X_j=0$ and vertex B such that $X_j=1$. Consider $f_i(X_1, X_2, \ldots, X_n)$ with the-variables $\{X_j\}$ set to the values of vertex A. If $f_i < \theta_i$ the edge is directed from vertex B to A; if $f_i > \theta_i$ the edge is directed from A to B. Further, attracting cycles in the state transition diagram imply the existence of a stable limit cycle attractor for some choice of the f_i and attracting vertices imply a stable fixed point [9]. Although Eq. (3) is not a monotonic equation since derivatives will be 0 except at the threshold hyperplanes, by substituting steep sigmoidal functions for step functions, we can generate monotonic networks that are described by both symbolic methods [10–13]. We now consider different networks satisfying the interaction diagram in Fig. 1(a) and show that the dynamics depends on the nature of the interactions between x_1 and x_3 in the activation of x_2.

First consider the case when $\alpha=0$ in Fig. 1(a) leading to a negative feedback network [4,9,14]. For this situation the state transition diagram is in Fig. 2(a) corresponding to the Boolean truth table

X_1	X_2	X_3	f_1	f_2	f_3
0	0	0	1	0	0
0	0	1	0	0	0
0	1	0	1	0	1
0	1	1	0	0	1
1	0	0	1	1	0
1	0	1	0	1	0
1	1	0	1	1	1
1	1	1	0	1	1

(4)

There is an attracting oscillation in the state transition diagram. The truth table implies that a piecewise linear differential equation of the form of Eq. (3) can be written for this system by use of the Heaviside function, $H(x-\theta)$, where $H=0$ for $x<\theta$ and $H=1$ for $x \geq \theta$.

In order to generate a continuous nonlinear monotone equation for this network, we use procedures sketched out previously and substitute the sigmoidal Hill function $S^+(x) = x^\eta/(\theta^\eta + x^\eta)$ for the Heaviside function, where η is called the Hill coefficient [10]. As $\eta \to \infty$ the Hill function approaches the Heaviside function. In what follows, we arbitrarily select $\eta=5$ and $\theta=0.5$. The associated differential equation is

$$\dot{x}_1 = -x_1 + 1 - S^+(x_3),$$

$$\dot{x}_2 = -x_2 + S^+(x_1),$$

$$\dot{x}_3 = -x_3 + S^+(x_2). \quad (5)$$

Figure 2(b) shows an example of a transient dynamics approaching a stable limit cycle oscillation. The symbolic sequence using the derivative discretization is $(+-+) \to (--+) \to (---) \to (+--) \to (++-) \to (+++) \to (-++) \to (--+) \to \ldots$ and the symbolic sequence using threshold discretization ($\theta=0.5$) is $(010) \to (110) \to (111) \to (011) \to (001) \to (000) \to (100) \to (110) \to \ldots$. There is a supercritical Hopf bifurcation at $\eta=4$ [4,15], and in the limit, $\eta \to \infty$, there is a stable limit cycle oscillation [9].

If both 1 and 3 are needed to activate 2, f_2 would be an AND function and the state transition diagram is given in Fig. 3(a), corresponding to the AND truth table listed in Eq. (6).

Inputs			AND			OR		
X_1	X_2	X_3	f_1	f_2	f_3	f_1	f_2	f_3
0	0	0	1	0	0	1	0	0
0	0	1	0	0	0	0	1	0
0	1	0	1	0	1	1	0	1
0	1	1	0	0	1	0	1	1
1	0	0	1	0	0	1	1	0
1	0	1	0	1	0	0	1	0
1	1	0	1	0	1	1	1	1
1	1	1	0	1	1	0	1	1

(6)

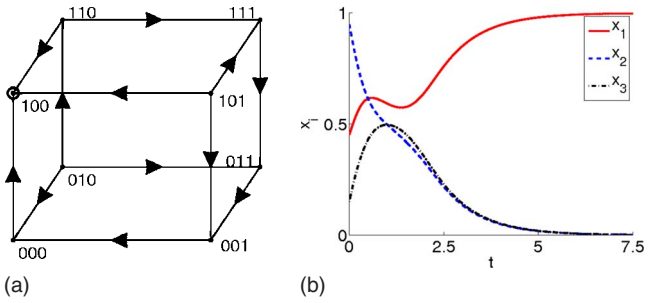

FIG. 3. (Color online) Analysis of Eq. (7) where both elements 1 and 3 are needed for activation of 2. (a) The state transition diagram showing allowed transitions between sectors (see text). (b) Numerical integration of Eq. (7) with $\eta=5$.

There is now a stable vertex at (100). The associated monotone differential equation is

$$\dot{x}_1 = -x_1 + 1 - S^+(x_3),$$

$$\dot{x}_2 = -x_2 + S^+(x_1)S^+(x_3),$$

$$\dot{x}_3 = -x_3 + S^+(x_2). \tag{7}$$

Figure 3(b) shows an example of a transient dynamics approaching a stable fixed point. Using the derivative discretization the sequence for the symbolic dynamics is $(+-+)\rightarrow(--+)\rightarrow(---)\rightarrow(+--)$. Using the threshold discretization with the threshold value $\theta=0.5$, then the symbolic states are $(010)\rightarrow(110)\rightarrow(100)$. The symbolic state sequence can be sensitive to the threshold values chosen. For instance, with $\theta=0.49$ then two new intermediate transitions take place: $(010)\rightarrow(110)\rightarrow(111)\rightarrow(101)\rightarrow(100)$, which contains the transition $(111)\rightarrow(101)$ in violation of the state transition diagram in Fig. 3(a). This observation underscores a weakness of the state transition diagram in the threshold discretization method since it is only proven in the limit $\eta\rightarrow\infty$.

Finally, if either 1 or 3 suffices to activate 2, f_2 would be an OR function and the state transition diagram is given in Fig. 4(a), corresponding to the OR truth table in Eq. (6). There is now a stable vertex at (011) and the monotone differential equation system is

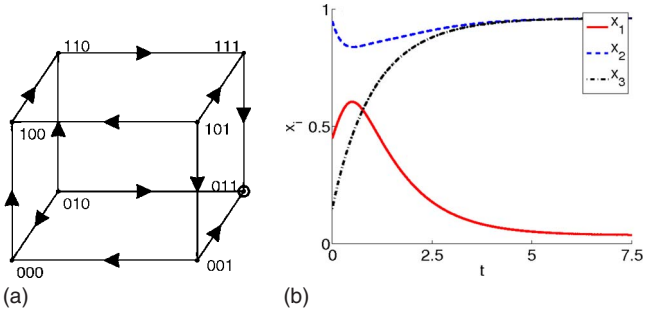

FIG. 4. (Color online) Analysis of Eq. (8) where activators 1 and 3 act independently on x_2. (a) The state transition diagram showing allowed transitions between sectors (see text). (b) Numerical integration of Eq. (8) with $\eta=5$.

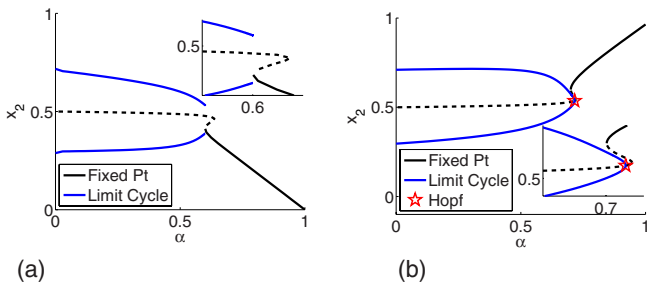

FIG. 5. (Color online) Bifurcation analysis of the AND system (a) and the OR system (b) using the numerical bifurcation tool AUTO-07p [16]. The insets are magnifications near the bifurcations as α varies. A saddle-node homoclinic bifurcation occurs for the AND case and a supercritical Hopf bifurcation for the OR one.

$$\dot{x}_1 = -x_1 + 1 - S^+(x_3),$$

$$\dot{x}_2 = -x_2 + S^+(x_1) + S^+(x_3) - S^+(x_1)S^+(x_3),$$

$$\dot{x}_3 = -x_3 + S^+(x_2). \tag{8}$$

Figure 4(b) shows an example of a transient dynamics approaching a stable fixed point. The sequence for the symbolic transitions during the transient are $(+-+)\rightarrow(--+)\rightarrow(-++)$ and $(010)\rightarrow(110)\rightarrow(111)\rightarrow(011)$.

Unlike in the AND case, the symbolic states using the threshold discretization are very robust to the threshold choice ($\theta_i=0.5$) when a finite η is used in Eq. (8).

These results do not give information about the robustness of the dynamics under parametric changes. To do this, we now vary the strength of the feedback loop $3\rightarrow2$ and show the bifurcation diagram for two situations found by substituting two different equations for x_2 in Eq. (5),

$$\dot{x}_2 = -x_2 - \alpha S^+(x_1)[1 - S^+(x_3)] + S^+(x_1) \quad \text{AND},$$

$$\dot{x}_2 = -x_2 + \alpha[1 - S^+(x_1)]S^+(x_3) + S^+(x_1) \quad \text{OR}, \tag{9}$$

In these equations, when $\alpha=0$ we have Eq. (5); and when $\alpha=1$ we have Eq. (7) using the AND function or Eq. (8) using the OR function. Figure 5 shows the bifurcation diagram for both these situations. Both the limit cycle and the fixed point behaviors prevail over a large range of the α parameter. For the AND function as α increases from 0 to 1, a saddle-node homoclinic bifurcation occurs. The stable limit cycle collides with the center manifold of the fixed point at $\alpha\approx0.600$. For the OR function as α increases from 0 to 1 a Hopf bifurcation occurs at $\alpha\approx0.716$ resulting in the stable limit cycle becoming a stable fixed point. There is a small region of bistability before the stable upper branch emerges as the unique fixed point. The results in Fig. 5 demonstrate that differential equations embodying the monotone network in Fig. 1 can robustly show fixed point behavior as well as the limit cycle oscillation found in the negative feedback network resulting when the interaction $3\rightarrow2$ is eliminated.

In addition to placing restrictions on the observed dynamics for a given network, the symbolic dynamics approach can be used for the "inverse problem" i.e., to determine the qualitative interactions based on observed dynamics using either

the derivative discretization [8] or the threshold discretization [17–19]. However, for a given unknown network, it may in general be difficult to know *a priori* if the network is monotone, as required by the derivative discretization method, or if the network embodies strong switchlike nonlinearities, as required by the threshold discretization.

There are some strong similarities and differences between the two symbolic dynamics approaches. The allowed symbolic transitions found using the derivative discretization applies for all networks displaying the same monotone structure [8], whereas the state transition diagram using the threshold discretization applies to the piecewise linear networks in Eq. (3) and continuous nonlinear networks that are sufficiently close to the piecewise linear equations [10–13]. Some piecewise linear networks, such as those in which a single variable could be an activator or an inhibitor depending on the values of other variables of the network, are not monotone and therefore cannot be analyzed using the derivative discretization. Other networks are monotone, but do not contain switchlike nonlinearities, and therefore cannot be analyzed using the threshold discretization. However, some networks, such as those described in Figs. 2–5 can be analyzed using both the derivative and threshold discretizations. For such networks, if each element receives only a single input from another element in the network the state transition diagrams using the different approaches will be identical. However, when there are multiple inputs to each element the state transition diagrams using the two approaches may be different, but the transitions using the threshold discretization will be a subset of those using the derivative discretization. This arises because all transitions involving a change in the sign derivative must be consistent with those determined using the derivative discretization, but not all transitions in the state transition diagram need occur in any particular monotone network. In contrast, all transitions in the state transition diagram using the threshold discretization can be observed in some region of phase space. As a consequence, using the threshold discretization, it is sometimes possible to derive precise information about detailed dynamics including prediction of some types of fixed points and cycles. Since numerous technical challenges arise when passing from the piecewise linear equations to continuous equations with steep sigmoidal nonlinearities [10–13], further study and rigorous mathematical analysis is needed. In conclusion, the complementary symbolic dynamics methods described here provide powerful tools for analyzing biological regulatory systems and for determining qualitative information about the biochemical interactions based on observed dynamics.

We thank NSERC for financial support and the reviewers for helpful comments.

[1] G. Lahav, N. Rosenfeld, A. Sigal, N. Geva-Zatorsky, A. J. Levine, M. B. Elowitz, and U. Alon, Nat. Genet. **36**, 147 (2004).
[2] D. B. Chklovskii, T. Schikorski, and C. F. Stevens, Neuron **34**, 341 (2002).
[3] D. A. Lind and B. Marcus, *An Introduction to Symbolic Dynamics and Coding* (Cambridge University Press, Cambridge, England, 1995).
[4] L. Glass, J. Chem. Phys. **63**, 1325 (1975).
[5] R. Thomas and R. D'Ari, *Biological Feedback* (CRC, Boca Raton, FL, 1990).
[6] R. Edwards, H. T. Siegelmann, K. Aziza, and L. Glass, Chaos **11**, 160 (2001).
[7] S. Pigolotti, S. Krishna, and M. H. Jensen, Proc. Natl. Acad. Sci. U.S.A. **104**, 6533 (2007).
[8] S. Pigolotti, S. Krishna, and M. H. Jensen, Phys. Rev. Lett. **102**, 088701 (2009).
[9] L. Glass and J. S. Pasternack, J. Math. Biol. **6**, 207 (1978).
[10] L. Glass and J. S. Pasternack, Bull. Math. Biol. **40**, 27 (1978).
[11] E. Plahte, T. Mestl, and S. W. Omholt, Dyn. Stabil. Syst. **9**, 275 (1994).
[12] E. Plahte and S. Kjøglum, Physica D **201**, 150 (2005).
[13] S. Veflingstad and E. Plahte, Biosystems **90**, 323 (2007).
[14] M. Elowitz and S. Leibler, Nature (London) **403**, 335 (2000).
[15] W. F. Langford, Numer. Math. **28**, 171 (1977).
[16] E. J. Doedel *et al.*, *AUTO-07P: Continuation and Bifurcation Software for Ordinary Differential Equations* (Concordia University, Montreal, 2006).
[17] T. J. Perkins, M. Hallett, and L. Glass, J. Theor. Biol. **230**, 289 (2004).
[18] S. Drulhe, G. Ferrari-Trecate, H. De Jong, and A. Viari, Lect. Notes Comput. Sci. **3927**, 184 (2006).
[19] R. Wilds and L. Glass, Int. J. Bifurcation Chaos (to be published)